EDMS Document Number: 1406467

**ORGANISATION EUROPENNE POUR LA RECHERCHE NUCLEAIRE**
**EUROPEAN ORGANIZATION FOR NUCLEAR RESEARCH**
Laboratoire Européen pour la Physique des Particules
European Laboratory for Particle Physics

**Occupational Health & Safety and Environmental Protection Unit**

*Technical Note*
CERN–RP–2014–065–REPORTS–TN
29 August 2014

# Computation of radioactivity in particle accelerators and propagation of uncertainties with the JEREMY code

R. Froeschl, M. Magistris, F. Leite Pereira, C. Theis

*Summary*

Beam losses are responsible for material activation in certain components of particle accelerators. The activation is caused by several nuclear processes and varies with the irradiation history and the characteristics of the material (namely chemical composition and size). The maintenance, transport and elimination of the activated components requires their radiological characterization.

The JEREMY code computes the induced radioactivity from the fluence spectra of the radiation field to which the component of interest is exposed, from the irradiation history and from the chemical composition of the material. This paper presents the mathematical formulation of the computation of the induced activity including a detailed discussion of the propagation of the uncertainties on the induced radioactivity.



# 1 Introduction

The accelerator complex of the European Laboratory for Particle Physics (CERN) in Geneva has been operated for more than 50 years. The interaction of the particle beams with the accelerator components leads to the production of radioactive isotopes. The induced radioactivity has to be measured or calculated in order to plan maintenance operation, distinguish between conventional and radioactive material, transport it and select the appropriate elimination path.

The approach chosen for the computation of the induced radioactivity with the JEREMY code is based on two steps. First, the particle spectra of the radiation environment are calculated via Monte Carlo simulations with codes like FLUKA [1], Geant4 [2] or MCNPX [3]. Given these fluence spectra as input, the radioactivity build–up and subsequent decay are calculated with the JEREMY code for each isotope of interest. Previously developed algorithms for the computation of the radionuclide inventory at the Paul Scherrer Institute (PSI, Villigen, Switzerland) [4,5] (focused on neutron activation) and at CERN [6,7] have been extended and implemented in the JEREMY code.

This paper states the assumptions on which the computation performed with the JEREMY code is based. The mathematical formulation of the activity calculations is presented with a detailed discussion of the propagation of uncertainties on input parameters (e.g. irradiation history, material composition, fluence spectra and isotope production cross sections). Finally, the implementation of JEREMY is discussed.

Since the assumptions made in the two–step approach may be valid for problems other than the computation of the induced radioactivity of accelerator components, the use of the JEREMY code can be extended to other fields, e.g. structural material in nuclear reactors.

# 2 Assumptions

This section describes the assumptions on which the radiological characterization calculated with the JEREMY code is based.

## 2.1 Irradiation history

The irradiation history is a critical input parameter for the computation of the induced activity. In this paper, the computation of the induced activity is described for an irradiation profile that can be considered as constant on time scales larger than the half life of the shortest–lived nuclide of interest. This constant irradiation period of length $t_{\mathrm{irr}}$ is followed by a cooling period of duration $t_{\mathrm{cool}}$.

In the case of particle accelerators, the main source of the induced activity is beam loss. Since the beam loss profile should be more or less constant over time, the assumption of a constant irradiation profile is easily fulfilled for most CERN accelerator components.

However, the induced activity for an arbitrary irradiation profile can be computed by first approximating the irradiation profile with an irradiation histogram and then by the summation of the induced activities over the time slices of constant irradiation. In order to approximate the arbitrary irradiation profile sufficiently well, the time slices have to be chosen fine enough.

### 2.2 Particle spectra

The spectra for the activating particles of the radiation field have to be known for the waste item. With respect to the spatial location in the waste item, the most common cases can be identified as:

1. The size of the concerned waste item is small compared to the interaction lengths of the particle types and energies that are dominant in the activation process. Therefore the particle spectra can be considered as uniform and the computed specific activity is homogeneously distributed over the waste item.
2. The size of the concerned waste item is large compared to the interaction lengths of the particle types and energies that are dominant in the activation process. Therefore the particle spectra vary depending on the position in the waste item. Using a track length estimator, average particle energy fluence spectra can be scored. The specific activity obtained with these spectra is an average value for the whole waste item and provides no information on the spacial distribution of the specific activity.

Furthermote, the spectra for the activating particles of the radiation field have to be the same for the whole irradiation period. If this is not the case, the irradiation period must be divided into smaller parts until this condition is met or the remaining non–uniformity is taken into account by treating it as an uncertainty on the particle spectra.

Uncertainties on these spectra can be propagated to the computed induced radioactivity.

### 2.3 Uniform and known material composition

The material composition, i.e. the mass weight fractions of the chemical elements, must be uniform within the waste item. If this is not the case, the waste item must be divided into smaller parts until this condition is met or the remaining non–uniformity is taken into account by treating it as an uncertainty on the material composition.

Uncertainties on the material composition can be propagated to the computed induced radioactivity.

### 2.4 No interaction between the radiation field and the produced isotopes

No interaction between the radiation field and the isotopes produced during the irradiation period are taken into account. This means that the amount of nuclei of the isotopes produced during the irradiation period has to be very small compared to the amount of initial material of the component.

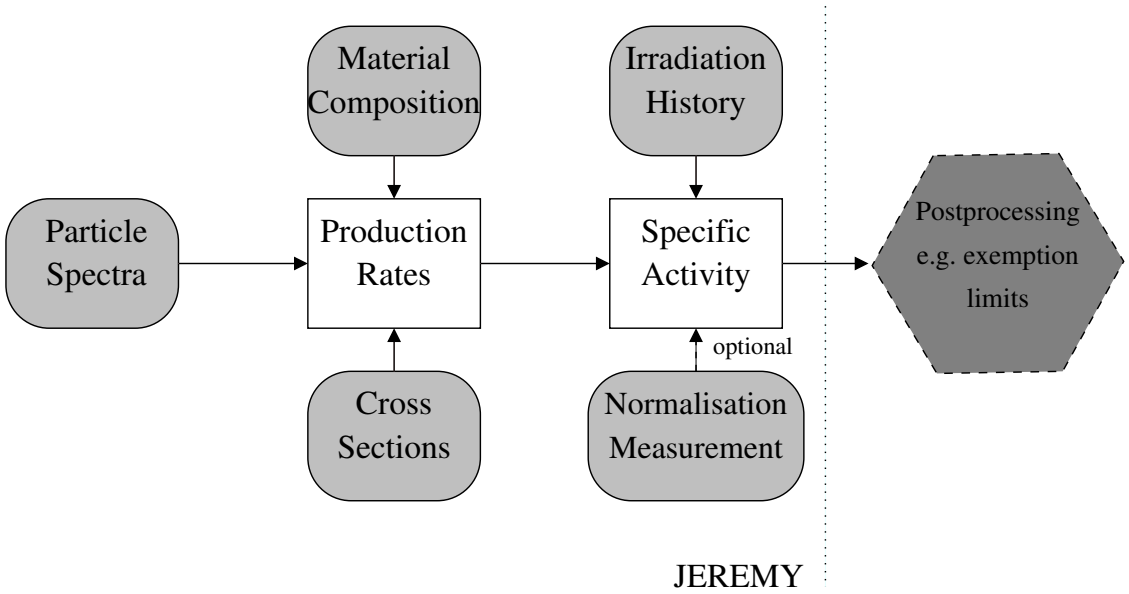


Figure 1: Flow of information within the JEREMY code for the computation of the induced activity.

### 2.5 No depletion of the initial material

It is assumed that there is no depletion of the initial material due to the interactions with the radiation field. This means that the amount of nuclei of the isotopes produced during the irradiation period has to be very small compared to the amount of initial material of the component. As a consequence, the capabilities of the JEREMY code to describe breeding reactions are very limited.

## 3 Computation of the induced specific activity

This section is devoted to the computation of the induced specific activity. After the description of the information flow within the JEREMY code in Sec. 3.1, the mathematical formulation of the computation of the induced specific activity is given in Sec. 3.2. The necessary input data are described in Sec. 3.3 and normalisation issues are discussed in Sec. 3.4.

### 3.1 Flow of information

The flow of information within the JEREMY code for the computation of the induced activity is shown in Fig. 1. The fluence spectra together with the isotope production cross sections as well as the material composition of the component are used to compute the *isotope production rates*. The *isotope production rates* together with the irradiation history yield the specific activity. In case a normalisation of the specific activity is needed (see Sec. 3.4), a dose rate measurement or the measurement of the specific activity of a certain gamma emitter can be used to obtain a proper normalised specific activity.

### 3.2 Matrix formalism

The specific activity of isotope $b$ induced by a loss rate of one primary beam particle per second is given by

$$A_b = \sum_r \sum_e T_{br}\ P_{re}\ m_e \tag{1}$$

where $m_e$ denotes the weight fraction for element $e$, $r$ denotes all isotopes that are directly produced and $e$ the elements of the material. The matrix $T_{br}$ describes the time evolution and is defined later (see Eq. 3).

The production rate of isotope $r$ from element $e$ for a loss rate of one primary beam particle per second is given by the matrix

$$P_{re} = \frac{N_A}{M_e} \sum_{i=\mathrm{p,n},\gamma,\pi^+,\pi^-} \int \Phi_i(E)\, \sigma_{i,e,r}(E)\, dE \tag{2}$$

where $N_A$ is Avogadro's constant and $M_e$ is the atomic weight for the element $e$. The sum is extended over protons ($p$), neutrons ($n$), charged pions ($\pi^+, \pi^-$) and photons ($\gamma$). In this formulation, the natural isotope abundances for each element $e$ are taken into account, i.e. the cross section $\sigma_{i,e,r}(E)$ is an abundance weighted average of the cross sections of each isotope of element $e$. Furthermore, $\Phi_i(E)$ denotes the radiation fluence for the various secondary particles ($i = \mathrm{p, n}, \gamma, \pi^+, \pi^-$) generated by one primary beam particle per second. The expression $\sum_e P_{re}\ m_e$ corresponds to the production rate of isotope $r$ in the whole component for a loss rate of one primary beam particle per second.

The time evolution of the specific activity of isotope $b$, i.e. the build–up of isotope $r$ and the full decay chain leading to isotope $b$, is described by the matrix $T_{br}$. For an irradiation profile of a constant irradiation period of duration $t_{\mathrm{irr}}$ followed by a cooling time of duration $t_{\mathrm{cool}}$, the time evolution $T_{br}$ is given by

$$\begin{aligned} T_{br}(t_{\mathrm{irr}}, t_{\mathrm{cool}}) &= \sum_{c,r\to b} \int_0^{t_{\mathrm{irr}}} \sum_{m=1}^{j_c} c_m^c\, e^{-\lambda_m^c\,((t_{\mathrm{cool}}+t_{\mathrm{irr}})-t_0)}\, dt_0 \\ &= \sum_{c,r\to b} \sum_{m=1}^{j_c} \frac{c_m^c}{\lambda_m^c} \left( e^{-\lambda_m^c\, t_{\mathrm{cool}}} - e^{-\lambda_m^c\,(t_{\mathrm{cool}}+t_{\mathrm{irr}})} \right) \\ &= \sum_{c,r\to b} \sum_{m=1}^{j_c} \frac{c_m^c}{\lambda_m^c}\, e^{-\lambda_m^c\, t_{\mathrm{cool}}} \left( 1 - e^{-\lambda_m^c\, t_{\mathrm{irr}}} \right) \end{aligned} \tag{3}$$

where $c$ runs over all decay chains starting from isotope $r$ leading to isotope $b$ and $j_c$ is the number of isotopes in a given decay chain $c$. $\lambda_m^c$ denotes the total decay rate of the m$^{\mathrm{th}}$ isotope in decay chain $c$. $\tilde{\lambda}_m^c$ denotes the partial decay rate of the m$^{\mathrm{th}}$ isotope in the given decay chain $c$ and the coefficient $c_m^c$ is the *bateman coefficient* [8,9] of the m$^{\mathrm{th}}$ isotope in decay chain $c$ given by

$$c_m^c = \frac{\prod_{i=1}^{j_c} \tilde{\lambda}_i^c}{\prod_{\substack{i=1 \\ i\neq m}}^{j_c} (\lambda_i^c - \lambda_m^c)}. \tag{4}$$

In order to avoid numerical instabilities in Eq. 3 and 4, these expressions might be evaluated in multiple-precision arithmetic.

The computation of the time evolution for arbitrary irradiation profiles is discussed in Sec. 2.1.

### 3.3 Input data

The fluence spectra for various secondary particles, mainly $\mathrm{p}, \mathrm{n}, \gamma, \pi^+$ and $\pi^-$, per primary beam particle are critical inputs for the calculation of the induced activity. They can be obtained by Monte Carlo simulations with codes like FLUKA [1], Geant4 [2] or MCNPX [3].

The isotope production cross sections are also needed. For JEREMY, the isotope production cross sections for neutrons below $20\,\mathrm{MeV}$ have been extracted from the JEFF 3.1.1 library [10] including the energy dependent branching ratios between ground state and isomeric states when available. The isotope production cross sections for neutrons above $20\,\mathrm{MeV}$ as well as for $\mathrm{p}, \pi^+$ and $\pi^-$ have been calculated with FLUKA [11] where a branching ratio of 50%/50% between ground state and the first isomeric state has been assumed for isotopes with isomeric states. The isotope production cross sections for photons up to $200\,\mathrm{MeV}$ have been extracted from the TENDL2010 library [12] that is based on the TALYS code.

The decay data used in JEREMY has been extracted from the JEFF 3.1.1 library [10]. No time cut–off is applied in the time evolution, even for very short lived isotopes.

### 3.4 Normalisation

If the absolute scale of the flux of primary particles is not known, the computed specific activity has to be normalised. There are several normalisation methods, including the normalisation to a dose rate measurement [6] or to the activity of a certain gamma emitter [7].

## 4 Error propagation

Standard error propagation assuming Gaussian errors with a given covariance matrix can be used to estimate the uncertainty of the induced activity. For this method, the derivatives with respect to the parameters of interest are required. This sections describes the computation of the derivation with respect to the material composition (Sec. 4.1), to the parameters describing the irradiation history (Sec. 4.2) and to the particle spectra and the isotope production cross sections (Sec. 4.3). The error estimation is discussed in Sec. 4.4 for the induced activity and in Sec. 4.5 for derived quantities.

The uncertainty of the induced activity can also be estimated by means of dedicated Monte Carlo simulations. This approach is presented in Sec. 4.6.

### 4.1 Material composition

The derivative of the induced activity (Eq. 1) with respect to $m_e$ is given by

$$\frac{\partial A_b}{\partial m_e} = \sum_r T_{br} \, P_{re}. \tag{5}$$

### 4.2 Irradiation history

The derivative of the induced activity with respect to $t_{\mathrm{cool}}$ is given by

$$\frac{\partial A_b}{\partial t_{\mathrm{cool}}} = \sum_r \sum_e \frac{\partial T_{br}}{\partial t_{\mathrm{cool}}} \, P_{re} \, m_e \tag{6}$$

with

$$\frac{\partial T_{br}}{\partial t_{\mathrm{cool}}} = \sum_{c,r\to b} \sum_{m=1}^{j_c} -c_{m,c} \left( e^{-\lambda_{m,c} \, t_{\mathrm{cool}}} - e^{-\lambda_{m,c} \, (t_{\mathrm{cool}} + t_{\mathrm{irr}})} \right). \tag{7}$$

The derivative of the induced activity with respect to $t_{\mathrm{irr}}$ is given by

$$\frac{\partial A_b}{\partial t_{\mathrm{irr}}} = \sum_r \sum_e \frac{\partial T_{br}}{\partial t_{\mathrm{irr}}} \, P_{re} \, m_e \tag{8}$$

with

$$\frac{\partial T_{br}}{\partial t_{\mathrm{irr}}} = \sum_{c,r\to b} \sum_{m=1}^{j_c} c_{m,c} \, e^{-\lambda_{m,c} \, (t_{\mathrm{cool}} + t_{\mathrm{irr}})}. \tag{9}$$

### 4.3 Particle spectra and isotope production cross sections

Often, the particle spectra and the isotope production cross sections are only available as tabulated values, i.e. histograms. As a consequence, the integral of the folding of the particle spectrum and the isotope production cross section in Eq. 2 transforms into the sum

$$P_{re} = \frac{N_A}{M_e} \sum_{i=\mathrm{p,n},\gamma,\pi^+,\pi^-} \sum_{l=1}^{N_i} \Phi_i(l) \, \sigma_{i,e,r}(l) \, \Delta E_i(l) \tag{10}$$

provided that the binning of the spectrum histogram and the isotope production cross section histogram are identical for each particle type. The index $l$ iterates over the $N_i$ common bins for particle type $i$. If the binning of the spectrum histogram and the isotope production cross section histogram are not identical, these histograms are rebinned to a common binning. The new binborders, i.e. $\{\bar{q}_l\}_{l\in[0,N_i]}$, are the union of the binborders of the spectrum histogram and the binborders of the isotope production cross section histogram. The details of the rebinning including the calculation of the covariance matrix for the rebinned histograms are given in the Appendix.

Assuming that the common binning is described by the binborders $\{\bar{q}_{i,l}\}_{l\in[0,N_i]}$, the derivative of the induced activity with respect to the l-th bin $\Phi_i(l)$ of the spectrum histogram is given by

$$\frac{\partial A_b}{\partial \Phi_i(l)} = \sum_r \sum_e T_{br} \, \frac{\partial P_{re}}{\partial \Phi_i(l)} \, m_e, \tag{11}$$

where

$$\frac{\partial P_{re}}{\partial \Phi_i(l)} = \frac{N_A}{M_e}\,\sigma_{i,e,r}(l)\,\Delta E_i(l), \tag{12}$$

with $\Delta E_i(l) = \bar{q}_{i,l+1} - \bar{q}_{i,l}$.

The derivative of the induced activity with respect to the l-th bin $\sigma_{i,e,r}(l)$ of the isotope production cross section histogram for isotope $r$ by shooting particle type $i$ onto element $e$ is given by

$$\frac{\partial A_b}{\partial \sigma_{i,e,r}(l)} = \sum_r \sum_e T_{br}\,\frac{\partial P_{re}}{\partial \sigma_{i,e,r}(l)}\,m_e, \tag{13}$$

where

$$\frac{\partial P_{re}}{\partial \sigma_{i,e,r}(l)} = \frac{N_A}{M_e}\,\Phi_i(l)\,\Delta E_i(l). \tag{14}$$

### 4.4 Error on the induced activity

In most cases, the irradiation history, material composition, the particle spectra and the isotope production cross sections will not be pair–wise correlated apart from the material composition and the particle spectra. However, the impact of small changes in the material composition on the particle spectra will be very low in general.

Neglecting this small impact, the variance of the induced activity is therefore given by

$$\begin{aligned}\sigma^2_{A_b} = &\sum_{t_i,t_j=t_{\text{cool}},t_{\text{irr}}} \frac{\partial A_b}{\partial t_i}\,\sigma_{t_i,t_j}\,\frac{\partial A_b}{\partial t_j} + \sum_{m_{e_i},m_{e_j}} \frac{\partial A_b}{\partial m_{e_i}}\,\sigma_{m_{e_i},m_{e_j}}\,\frac{\partial A_b}{\partial m_{e_j}} + \\ &\sum_{i=\text{p,n},\gamma,\pi^+,\pi^-}\sum_{\Phi_i(l),\Phi_i(j)} \frac{\partial A_b}{\partial \Phi_i(l)}\,\sigma_{\Phi_i(l),\Phi_i(j)}\,\frac{\partial A_b}{\partial \Phi_i(j)} + \\ &\sum_r\sum_e\sum_{i=\text{p,n},\gamma,\pi^+,\pi^-}\sum_{\sigma_{i,e,r}(l),\sigma_{i,e,r}(j)} \frac{\partial A_b}{\partial \sigma_{i,e,r}(l)}\,\sigma_{\sigma_{i,e,r}(l),\sigma_{i,e,r}(j)}\,\frac{\partial A_b}{\partial \sigma_{i,e,r}(j)}\end{aligned} \tag{15}$$

where $\sigma_{t_i,t_j}$ is the covariance matrix of $t_{\text{cool}}$ and $t_{\text{irr}}$, $\sigma_{m_{e_i},m_{e_j}}$ the covariance matrix for the material composition, $\sigma_{\Phi_i(l),\Phi_i(j)}$ the covariance matrix for the spectrum of particle type $i$ and $\sigma_{\sigma_{i,e,r}(l),\sigma_{i,e,r}(j)}$ the covariance matrix for the isotope production cross section for isotope $r$ by shooting particle type $i$ onto element $e$.

Since the derivatives involved in the computation of the variance on the induced activity are available to the user, the impact of the uncertainty of single input parameter, e.g. the cooling time $t_{\text{cool}}$ or the cross section for a specific process, on the total variance on the induced activity can be assessed.

### 4.5 Error on derived quantities

The uncertainties can be propagated further for derived quantities since the derivatives involved in the computation of the variance on the induced activity are available to the user. This is illustrated for the computation of the exemption limit value according to the Swiss legislation (which

is a weighted sum of the specific activities). Furthermore it is assumed that the nuclide inventory has been normalised to the measured specific activity of $^{60}$Co, denoted $A^{\mathrm{m}}_{^{60}\mathrm{Co}}$, before. This yielded a normalisation factor of $A^{\mathrm{m}}_{^{60}\mathrm{Co}}/A^{\mathrm{p}}_{^{60}\mathrm{Co}}$ where $A^{\mathrm{p}}_{^{60}\mathrm{Co}}$ is the specific activity of $^{60}$Co predicted by JEREMY before normalisation. The normalised specific activity for a certain isotope $b$ is then given by

$$A_b^{\mathrm{norm}} = \frac{A^{\mathrm{m}}_{^{60}\mathrm{Co}}}{A^{\mathrm{p}}_{^{60}\mathrm{Co}}}\, A_b^{\mathrm{p}}, \tag{16}$$

where $A_b^{\mathrm{p}}$ is the specific activity of isotope $b$ predicted by JEREMY before normalisation. The exemption limit value LE is the sum over all isotopes where each isotope $b$ is weighted with a predefined factor $\mathrm{LE}_b$

$$\mathrm{LE} = \sum_b \frac{A_b^{\mathrm{norm}}}{\mathrm{LE}_b} = \frac{A^{\mathrm{m}}_{^{60}\mathrm{Co}}}{A^{\mathrm{p}}_{^{60}\mathrm{Co}}} \sum_b \frac{A_b^{\mathrm{p}}}{\mathrm{LE}_b}. \tag{17}$$

The derivative of LE with respect to the measured specific activity of $^{60}$Co $A^{\mathrm{m}}_{^{60}\mathrm{Co}}$ is simply given by

$$\frac{\partial\,\mathrm{LE}}{\partial\, A^{\mathrm{m}}_{^{60}\mathrm{Co}}} = \frac{1}{A^{\mathrm{p}}_{^{60}\mathrm{Co}}} \sum_b \frac{A_b^{\mathrm{p}}}{\mathrm{LE}_b}. \tag{18}$$

To provide a second example, the derivative of LE with respect to $t_{\mathrm{cool}}$ is given by

$$\begin{aligned}
\frac{\partial\,\mathrm{LE}}{\partial\, t_{\mathrm{cool}}} =& \frac{\partial}{\partial\, t_{\mathrm{cool}}} \left(\frac{A^{\mathrm{m}}_{^{60}\mathrm{Co}}}{A^{\mathrm{p}}_{^{60}\mathrm{Co}}}\right) \sum_b \frac{A_b^{\mathrm{p}}}{\mathrm{LE}_b} + \frac{A^{\mathrm{m}}_{^{60}\mathrm{Co}}}{A^{\mathrm{p}}_{^{60}\mathrm{Co}}} \sum_b \frac{\frac{\partial}{\partial\, t_{\mathrm{cool}}} A_b^{\mathrm{p}}}{\mathrm{LE}_b} \\
=& -\frac{A^{\mathrm{m}}_{^{60}\mathrm{Co}}}{\left(A^{\mathrm{p}}_{^{60}\mathrm{Co}}\right)^2} \sum_r \sum_e \left(\frac{\partial\, T_{^{60}\mathrm{Co}\,r}}{\partial\, t_{\mathrm{cool}}}\right) P_{re}\, m_e \cdot \sum_b \frac{A_b^{\mathrm{p}}}{\mathrm{LE}_b} + \\
& \frac{A^{\mathrm{m}}_{^{60}\mathrm{Co}}}{A^{\mathrm{p}}_{^{60}\mathrm{Co}}} \sum_b \frac{\left(\frac{\partial\, T_{br}}{\partial\, t_{\mathrm{cool}}}\right) P_{re}\, m_e}{\mathrm{LE}_b},
\end{aligned} \tag{19}$$

where the definition of $A_b^{\mathrm{p}}$ (Eq. 1) has been used. The derivative $\partial\, T_{br}/\partial\, t_{\mathrm{cool}}$ is given in Eq. 7. The variance on the exemption limit value LE is then computed similar to the variance of the induced activity (Sec. 4.4, Eq. 15) by exchanging $A_b$ for LE and the addition of the term $\left(\frac{\partial\, T_{br}}{\partial\, t_{\mathrm{cool}}}\right)^2 \sigma^2_{A^{\mathrm{m}}_{^{60}\mathrm{Co}}}$ that takes the uncertainty $\sigma_{A^{\mathrm{m}}_{^{60}\mathrm{Co}}}$ of the measured specific activity of $^{60}$Co into account.

In the JEREMY code, the propagation of the uncertainties is implemented for the two normalisation methods mentioned in Sec. 3.4. Furthermore, the user is able to propagate the uncertainties for arbitrarily complex arithmetic expressions via the scripting interface (see Sec. 5).

### 4.6 Monte Carlo simulation

Another possible way to estimate the uncertainty of the induced activity is to attribute a probability density distribution to every parameter of interest. These probability density distributions are used to perform a Monte Carlo simulation which yields a distribution for the induced activity $A_b$. This approach has also been implemented in JEREMY.

Since the induced activities $A_b$ are available to the user at an event–by–event base, the distributions of derived quantities can easily be obtained.

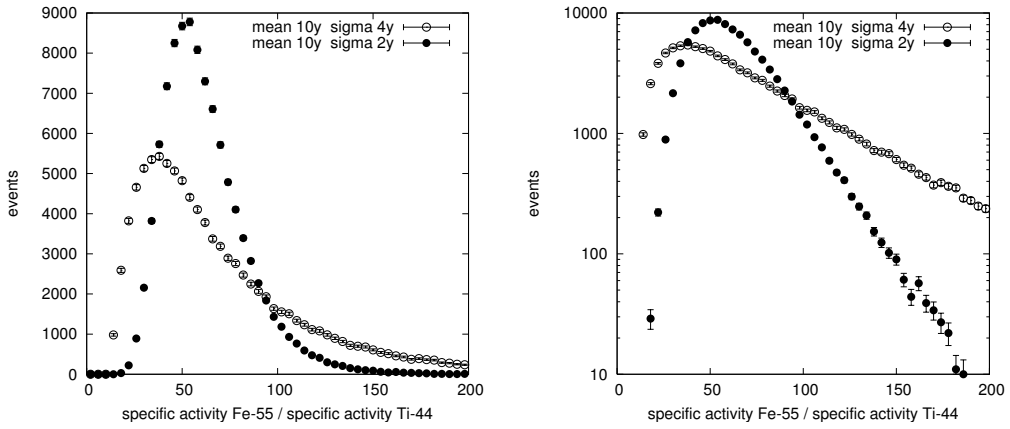


(a) linear scale (b) logarithmic scale

Figure 2: Distribution of the ratio of the specific activities of $^{55}$Fe and $^{44}$Ti obtained with JEREMY Monte Carlo simulations for two different irradiation histories. The irradiation histories are described in the text.

As an example for the estimation the uncertainty arising from the uncertainty of the irradiation history using Monte Carlo simulations, the distribution of the ratio of the specific activities of $^{55}$Fe and $^{44}$Ti is shown in Fig. 2 for two different irradiation histories. For the first irradiation history, the irradiation time $t_{\mathrm{irr}}$ is distributed as a Gaussian with a mean of 10 years and a standard deviation of 4 years. For the second irradiation history, the irradiation time $t_{\mathrm{irr}}$ is also distributed as a Gaussian with a mean of 10 years but with a standard deviation of only 2 years. For both irradiation histories the sum of the irradiation time $t_{\mathrm{irr}}$ and the cooling time $t_{\mathrm{cool}}$ is set to 34 years. The isotope production rates have been computed from spectra of the radiation field of the CERN SPS (Super Proton Synchrotron) and can be considered as arbitrary since they only influence the scale of the $x$ axis in Fig. 2. The distribution is asymmetric because the half-life of $^{55}$Fe is 2.73 years whereas half-life of $^{44}$Ti is 60 years. Indeed, a 2 year change in the cooling time has a significant impact on the specific activity of $^{55}$Fe and a negligible impact on the specific activity of $^{44}$Ti. The prediction of the ratio of the specific activities of $^{55}$Fe and $^{44}$Ti is important since $^{44}$Ti is a gamma emitter whose specific activity can be measured in–situ using gamma spectroscopy. On the other hand, $^{55}$Fe is an almost pure beta emitter whose specific activity is difficult to measure in–situ. The specific activity of $^{55}$Fe can be predicted by first computing the nuclide inventory with JEREMY and then scaling the whole nuclide inventory (including $^{55}$Fe) such that the predicted specific activity of $^{44}$Ti is equal to the measured one [7].

## 5 Implementation

The JEREMY code has been implemented in PYTHON [13] using the NumPy package [14]. Selected core routines have be optionally coded in ANSI C to reduce the computation time.

Because PYTHON is a scripting language and the JEREMY code has been implemented in PYTHON, JEREMY automatically provides a scripting interface to the user. Therefore it is rather simple to implement custom parameter distributions or dedicated post–processing routines for

example. Furthermore the user has full access to all computed quantities for further data exploration.

## 6 Conclusions

The JEREMY code computes the induced radioactivity from the fluence spectra of the radiation field generated by the beam loss. These fluence spectra are folded with isotope production cross sections obtained from FLUKA models [11] except for neutron below 20 $\mathrm{MeV}$ for which they have been taken from the JEFF 3.1.1 library [10].

The JEREMY code provides extensive uncertainty estimation capabilities using either error propagation assuming Gaussian errors or dedicated Monte Carlo simulations. For Gaussian error propagation, the full covariance matrices of the isotope production cross sections and of the fluence spectra are taken into account. For the estimation of the uncertainty of the induced radioactivity via dedicated Monte Carlo simulations, the uncertainty of input parameters can be modeled by arbitrarily complex probability density distributions.

The JEREMY code is fully exposed to the user in the PYTHON language. This facilitates in–depth data exploration since all quantities involved in the computation of the accelerator radiation induced activity are accessible to the user.

## Acknowledgments

We would like to thank A. Ferrari (CERN) and S. Roesler (CERN) for providing the cross sections calculated with FLUKA [11] for neutrons above 20 $\mathrm{MeV}$ as well as for protons and charged pions.

## References

[1] A. Ferrari, P. R. Sala, A. Fasso, and J. Ranft. *FLUKA: A multi-particle transport code (program version 2005)*. CERN, Geneva, 2005.

[2] S. Agostinelli et al. (GEANT4 Collaboration). Geant4: A simulation toolkit. *Nucl. Instrum. Meth.*, A506:250, 2003.

[3] H. G. Hughes, R. E. Preal, and R. .C Little. MCNPX - The LAHET/MCNP Code Merger. Technical Report LA-UR-97-4891, LANL, 1997.

[4] F. Atchison. Inventories for active-waste from accelerator facilities. Scientific and Technical Report 90, PSI, 2002. ISSN 1423-7650.

[5] S. Teichmann, M. Wohlmuther, and J. Züllig. Charakterisierung und Klassifizierung radioaktiver Abfälle aus den Beschleunigeranlagen des PSI. In *Fortschritte im Strahlenschutz: Strahlenschutzaspekte bei der Entsorgung radioaktiver Stoffe*, Basel, Switzerland, 2005. ISSN 1013-4506, 192.

[6] M. Magistris. The matrix method for radiological characterization of radioactive waste. *Nucl. Instrum. Methods Phys. Res., B*, 262:182–188, 2007.

[7] M. Magistris and L. Ulrici. The fingerprint method for characterization of radioactive waste in hadron accelerators. *Nucl. Instrum. Methods Phys. Res., A*, 591(2):343–352, 2008.

[8] H. Bateman. Solution of a system of differential equations occurring in the theory of radioactive transformations. *Proc. Cambridge Philos. Soc.*, 15:423–427, 1910.

[9] J. K. Shultis and R. E. Faw. *Fundamentals of nuclear science and engineering*. Dekker, Abingdon, 2002.

[10] A. Santamarina et al. The JEFF-3.1.1 Nuclear Data Library. Technical Report JEFF Report 22, Nuclear Energy Agency, Paris, 2009.

[11] A. Fasso, A. Ferrari, S. Roesler, P. R. Sala, F. Ballarini, A. Ottolenghi, G. Battistoni, F. Cerutti, E. Gadioli, M. V. Garzelli, A. Empl, and J. Ranft. The physics models of fluka: status and recent development. Technical Report hep-ph/0306267, SLAC, Stanford, CA, June 2003.

[12] D. Rochman and A. J. Koning. TENDL-2010: Reaching completeness and accuracy. JEF/DOC-1349, OECD/NEA, 2010.

[13] G. V. Rossum. *The Python Language Reference Manual*. Network Theory Ltd., September 2003.

[14] L. M. Surhone, M. T. Timpledon, and S. F. Marseken. *NumPy*. Betascript Publishing, July 2010.

# Appendix

This appendix describes the rebinning of a histogram including the computation of the covariance matrix mentioned in Sec. 4.3 for Eq. 10.

The histogram to be rebinned is assumed to consist of $M$ bins. This means that there are $\{h_i\}_{i\in[0,M-1]}$ bin values, $\{q_i\}_{i\in[0,M]}$ bin borders with $q_i < q_{i+1}$ and a covariance matrix $c_{i,j},\ i,j \in [0, M-1]$. This histogram is rebinned to $N$ bins ($N > M$) with binborders $\{\bar{q}_i\}_{i\in[0,N]}$ by adding new binborders, i.e. $\{q_i\}_{i\in[0,M]} \subset \{\bar{q}_i\}_{i\in[0,N]}$.

Then the values $\{\bar{h}_l\}_{l\in[0,N-1]}$ for the rebinned histogram are given by

$$\bar{h}_l = h_{i(l)} \tag{20}$$

where $i(l)$ denotes the bin $i(l)$ in the original histogram where the new bin $l$ is contained, i.e. $[\bar{h}_l, \bar{h}_{l+1}] \subseteq [h_{i(l)}, h_{i(l)+1}]$.

The covariance matrix for the rebinned histogram $\bar{c}_{j,k},\ j,k \in [0, N-1]$ is given by

$$\bar{c}_{j,k} = c_{i(j),i(k)} \sqrt{\frac{\Delta q_{i(j)}}{\bar{\Delta} q_j} \frac{\Delta q_{i(k)}}{\bar{\Delta} q_k}} \tag{21}$$

where $\bar{\Delta} q_j = \bar{q}_{j+1} - \bar{q}_j$ and $\Delta q_i = q_{i+1} - q_i$. Eq. 21 ensures that the correlation between bins remains unchanged while the errors are scaled assuming poissonian statistics, i.e. by the square root of the ratio of the bin widths.

Instead of selecting just the corresponding bin value of the original histogram as bin value for the rebinned histogram (Eq. 20) more sophisticated interpolation schemes could be chosen for increased numerical precision. However, the computation of the corresponding covariance matrix for the rebinned histogram is much more difficult and therefore time consuming in this case.